CORROSION RESISTANCE OF ALUMINIUM-MAGNESIUM ALLOYS FOR THE MARINE MARKET

Ronan DIF [1], Tim WARNER [1] and Guy-Michel RAYNAUD [2]

[1] Pechiney Centre de Recherches de Voreppe, BP 27, 38340 Voreppe, France
[2] Pechiney Rhenalu, Z.I. des Listes, BP 42, 63500 Issoire, France

ABSTRACT : A new Al-4.5%Mg alloy designated AA5383 has been developed by Pechiney Rhenalu. The intergranular, exfoliation and stress corrosion resistance of the new alloy and classical 5083 was characterised as a function of ageing. After ageing, the 5383 alloy exhibits a better resistance to intergranular and stress corrosion, and an equivalent behaviour as regards exfoliation. A mechanism that accounts for these results is proposed, based on thermodynamic calculations of equilibrium volume fraction of second phases and on TEM observations. Natural exposure trials were also conducted in the as-received state : they show that 5383 performs significantly better, which could be explained by its lower iron content and by a more elongated grain structure.

***Keywords** : Aluminium-Magnesium alloys, corrosion, pitting, exfoliation, intergranular, SCC*

1. INTRODUCTION

Aluminium sheets and plates of the Al-Mg series are extensively used in ship construction, more particularly for High Speed Light Craft. So far, most of the shipyards have almost exclusively used classical AA5083 which exhibits a good combination of mechanical strength, formability, weldability and corrosion resistance.

However, sensitisation to intergranular corrosion, exfoliation and/or stress corrosion cracking (SCC) of aluminium-magnesium alloys may occur after prolonged thermal exposure. The underlying mechanism of sensitisation is well documented (see [1] for example) : during ageing at temperatures below about 200°C, magnesium diffuses towards the grain boundaries and precipitates in the form of a thin film of the β-Al_3Mg_2 phase. In a standard saline solution, this phase is highly anodic with respect to the Al-Mg solid solution [2]. Provided that the film formed at the grain boundaries is continuous, it is oxidised in a microgalvanic coupling process which results in the rapid consumption of the Al_3Mg_2 grain boundary compound.

For this reason, the use of 5000 alloys with magnesium content exceeding 3.5 % is generally not recommended above 65°C. However, if exposure times are short enough or if the environment is only mildly aggressive, these alloys may be used at higher temperatures without any risk regarding structural corrosion.

Recently, a new alloy patented by Pechiney Rhenalu [3] and registered by the Aluminium Association as AA5383, involving optimised composition with respect to 5083, was developed (see [4] for example) in order to meet the requirements of improved mechanical strength after welding. The objective of this study is to compare the resistance to corrosion of 5083 and 5383 alloys and to investigate the mechanisms underlying the differences observed.

2. EXPERIMENTAL

6 mm thick sheets of commercial AA5083 and AA5383 were received in the H116 temper. The compositions as well as the yield strength of the two alloys obtained after welding are given in table 1. 5383, which has higher manganese and magnesium contents as well as a lower impurity level (iron and silicon) exhibits an improved yield strength after welding.

	Mg (wt %)	Mn (wt %)	Si (wt %)	Fe (wt %)	Cr (wt %)	Cu (wt %)	Zn (wt %)	Yield strength after welding (MPa)
5083	4.37	0.52	0.17	0.29	0.09	0	0.03	135
5383	4.58	0.76	0.08	0.15	0.12	0	0.06	155

Table 1 : Composition of the two alloys studied and yield strength after welding (weld bead-off).

In order to study the sensitisation to corrosion during thermal exposure of 5083 and 5383, several artificial ageing treatments were performed at temperatures ranging from 80 to 140°C.

Intergranular corrosion was evaluated through the so-called Interacid test [5] which is followed by measurements of the mass loss and depth of intergranular attack. The resistance to exfoliation was characterised by the procedure described in ASTM G66 ("ASSET" test).

The SCC susceptibility was assessed in the long-transverse direction by constant load alternate immersion tests in 3.5% NaCl at different stress levels ranging from 100 to 300 MPa according to ASTM G47. 3 specimens per case were tested. In addition to the static stress corrosion tests, slow strain rate experiments on 80 mm-gauge length specimens cut in the long-transverse direction were also conducted. The strain rate was 5.10^{-5} s^{-1} (4 µm/s cross-head speed) and the tests were performed at free potential in the laboratory air and in a 3%NaCl + 0.3%H_2O_2 solution. For each type of slow strain rate experiment, 3 samples were tested for statistical significance.

Finally, the resistance to corrosion in a natural marine environment situated on the mediterranean coast was determined by exposure of samples to marine atmosphere and immersion in sea water.

3. RESULTS

3.1. Intergranular and exfoliation corrosion

The evolution of the intergranular corrosion depth (Interacid test) as a function of ageing time and temperature is given in figure 1. The same type of behaviour could be obtained by considering the mass loss or the exfoliation results : the sensitivity to structural corrosion increases with time. The higher the temperature, the steeper the time-corrosion curve.

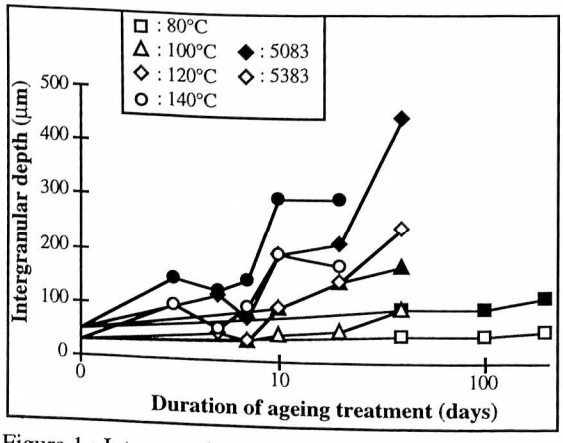

Figure 1 : Intergranular corrosion depth as a function of sensitisation time for different temperatures.

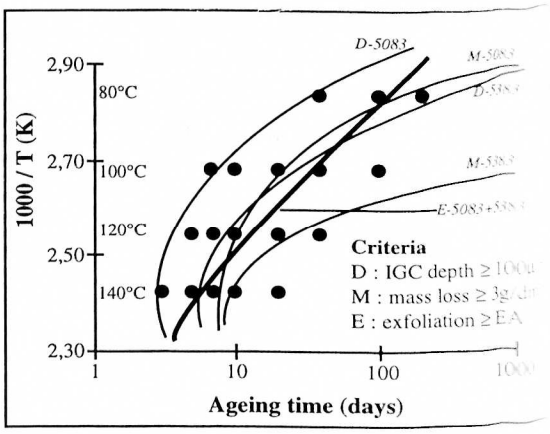

Figure 2 : Sensitisation diagrams for different corrosion tests and criteria.

An effective way of representing such sensitisation data consists of plotting the ageing treatments in a log(t)-1/T diagram [6]. A curve that separates the sensitive and unsensitive ageing conditions can then be drawn with respect to a given corrosion test and to a given sensitivity criterion. The sensitisation diagrams corresponding to different criteria are given in figure 2.

Without artificial sensitisation treatments, the two alloys tested are very resistant to intergranular and exfoliation corrosion. After ageing, 5383 performs clearly better than the classical 5083 with respect to intergranular corrosion. These two alloys have nevertheless the same resistance to exfoliation corrosion.

It is also noticeable that the sensitisation curves are not necessarily straight lines in a log(t)-1/T diagram. This means that the sensitisation phenomenon does not correspond to a simple thermal activation law. The complex shape of the sensitisation diagrams can be accounted for by the role of several temperature-dependant phenomena in the sensitisation mechanism (magnesium supersaturation entails its diffusion and precipitation). Supersaturation decreases as the ageing temperature increases. Diffusion is thermally activated but the activation energy depends on the diffusion mode (inside the grains, along the grain boundaries, through the sub-grains). Finally, the precipitation mode depends of the ageing temperature : intragranular precipitation is fostered as temperature increases and, above about 230°C, the β-Al_3Mg_2 phase precipitates in a discontinuous globular form.

3.2. Stress Corrosion Cracking

From the static SCC results performed on different ageing treatments at different stress levels, an estimation of the threshold stress for SCC can be derived. Neither of the two alloys is sensitive to SCC in the as-received temper, but it is clear from figure 3 that 5383 displays a much higher resistance to SCC than 5083 after artificial ageing.

As regards the dynamic SCC slow strain rate experiments, the aggressive solution can entail an extensive loss of ductility with respect to laboratory air. In order to ensure that this phenomenon is actually due to a synergistic action of stress and corrosion, some pre-exposure tests were also conducted. Three specimens of each alloy and ageing condition were tested in the laboratory air after immersion in the aggressive solution for the same duration as that of the tensile tests in NaCl + H_2O_2. It was shown that pre-exposure has no effect on ductility. The loss of ductility between air and the NaCl + H_2O_2 solution is therefore the result of "true" stress corrosion cracking. The sensitivity to SCC can thus be expressed as the elongation ratio R_{EI} :

$$R_{EI} = \frac{Elongation_{NaCl+H2O2}}{Elongation_{Air}}$$

A R_{EI} value of 1 (or 100%) stands for a high resistance to SCC. The ranking of the different alloys and ageing treatments as regards the R_{EI} ratio is given in figure 4. Again, there is a clear superiority of 5383 alloy. Observation by scanning electron microscopy of the fracture surfaces allows to distinguish between ductile and intergranular SCC failure. Taking for example the samples aged 40 days at 120°C and tested in the aggressive solution, there is twice as much intergranular surface for 5083 (40% of the total fracture surface) compared to 5383 (20%).

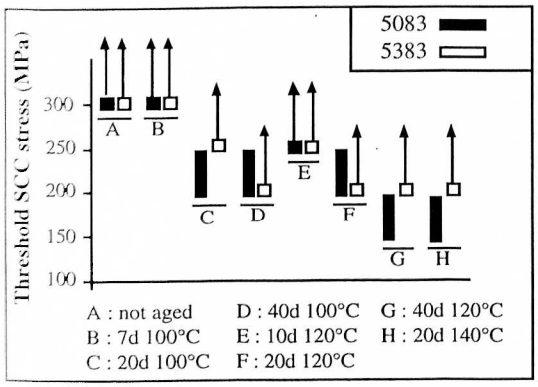

Figure 3 : Threshold SCC stress as a function of the alloy and ageing treatment. The bars give the range where the threshold is ; the arrows mean that the threshold is above the indicated value.

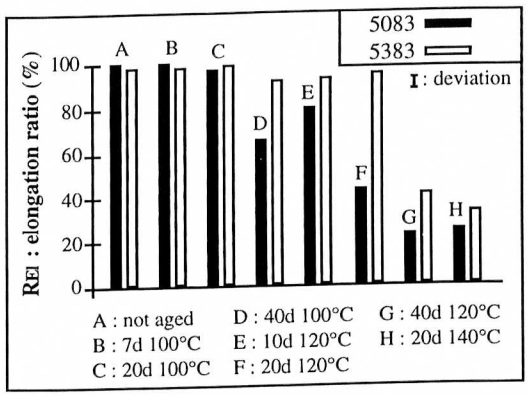

Figure 4 : Elongation ratio as a function of the alloy and ageing treatment.

3.3. Natural exposure tests

Optical micrographs of the corroded 5083 and 5383 samples display pitting corrosion but no evidence of either intergranular or exfoliation corrosion. Pit depths were measured optically on samples exposed to marine atmosphere (1 year), immersed in sea-water (1 and 2 years) or exposed

just above the sea line (1 and 2 years). We have given in figure 5, for each alloy and exposure condition, the maximum pit depth as well as the average depth of the five deepest pits. Data show that the pits are significantly shallower for 5383 after immersion and emersion exposures.

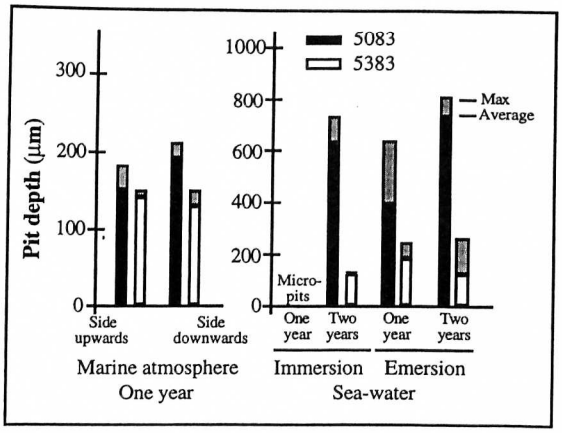

Figure 5 : Natural exposure results for 5083 and 5383 (average and maximum pit depths).

4. DISCUSSION

4.1. TEM observations

Samples of 5083 and 5383 were characterised in TEM in the as-received temper and after ageing treatments of 7 days at 100°C and 40 days at 120°C. No evidence of intergranular precipitation was found prior to ageing. However, in this as-received state, manganese-rich dispersoids were observed. For both alloys, image analysis of energy filtered images was combined with an estimation of the foil thickness in order to determine the characteristics (size and density) of these manganese-rich dispersoids. Results are given in table 2. The size and shape of the dispersoids are comparable for 5083 and 5383. Their density is however significantly higher for 5383.

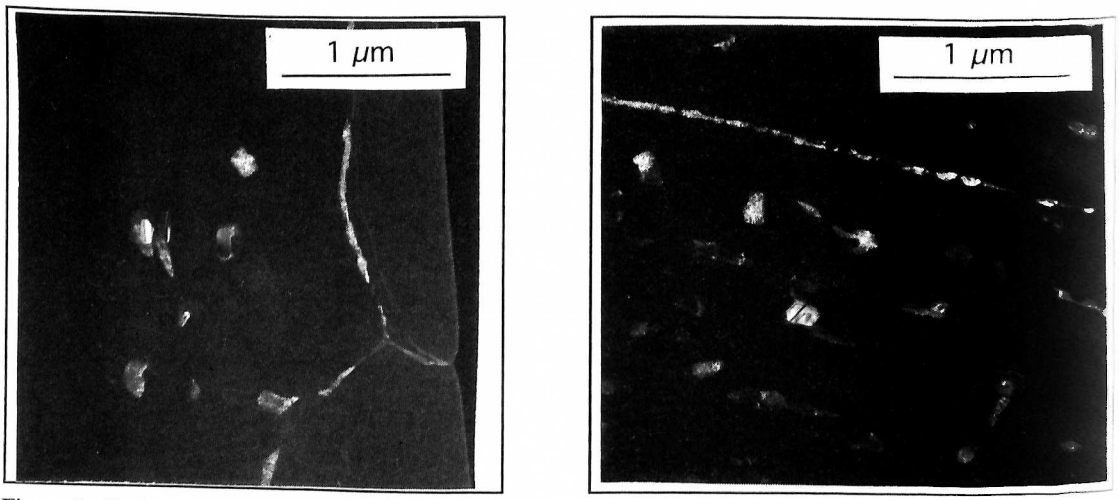

Figure 6 : Dark field images of the magnesium rich phase in 5083 (left) and 5383 (right) aged 40 days at 120°C. This phase is precipitated at the grain boundaries in the form of a continuous film. Note also the presence of these precipitates associated with manganese-rich dispersoids.

After ageing, both the grain boundaries and the manganese-containing dispersoids are decorated with a magnesium-rich phase (see figure 6). Also visible in these pictures are the manganese-containing dispersoids which are in some cases decorated with magnesium-rich precipitates.

4.2. Thermodynamic calculations

Calculations of the equilibrium volume fraction of dispersoids at 520°C (the pre-heat temperature before hot-rolling) were performed, using the model described by Sigli et al. [7]. These calculations take into account the trapping of manganese in the constituent particles (Al(Mn,Cr), Al_6(Mn,Fe) and Mg_2Si) as well as the solvus position at 520°C. As regards Al_6(Mn,Fe), the values quoted in table 2 correspond to the volume fraction of dispersoids at equilibrium, and are thus an overestimate of the true values, given the slow diffusion rate of manganese in aluminium. The calculated volume fraction of manganese-containing dispersoids is higher for 5383, which is consistent with the TEM observations.

	Calculated volume fraction (%)			TEM Measurements	
	Mg_2Si	Al_6(Fe,Mn)	Al(Cr,Mg)	Equivalent diameter (nm)	Number density (x 10^{18} m^{-3})
5083	0.6	0.63	0	154 ± 17	6.5 ± 0.3
5383	0.25	1.6	0.18	161 ± 14	10 ± 1.6

Table 2 : Thermodynamic calculation of the volume fraction of equilibrium phases and TEM characterisation of size and number density of the manganese-containing dispersoids.

4.3. Interpretation of the corrosion results

The new 5383 alloy clearly displays a higher resistance to intergranular corrosion after thermal exposure than 5083. By correlating this statement with the thermodynamic calculations and TEM observations, it is possible to imagine the underlying metallurgical mechanism. The main microstructural difference between 5083 and 5383 appears to be the number density of manganese-containing dispersoids. These dispersoids are competing sites for the precipitation of the β-Al_3Mg_2 phase : they may perturb the continuous grain boundary precipitation of this phase. Three types of interactions can be imagined : firstly, a dispersoid on a grain boundary can be the nucleation site for a globular precipitate, thereby breaking the continuity of the grain boundary decoration necessary for intergranular corrosion to take place. Secondly, the availability of alternative precipitation sites inside the grains will tend to disrupt magnesium diffusion towards grain boundaries. Thus, the more dispersoids in the alloy, the more the magnesium intergranular precipitation will be perturbed and the more resistant to intergranular corrosion the alloy will be. Finally, intragranular precipitation lowers the average potential of the grains, reducing the potential gap between grains and grain boundaries.

For Aluminium-Magnesium alloys, the mechanism for SCC is anodic grain boundary dissolution (i.e. intergranular corrosion) accelerated and assisted by the mechanical stress. Since 5383 is more resistant to intergranular corrosion than 5083, it is logical that its resistance to SCC is also enhanced.

Exfoliation corrosion is usually described as an intergranular corrosion phenomenon aggravated by an elongated grain structure. Given that 5383 contains more manganese-rich dispersoids that have an anti-recrystallisation effect, a more elongated grain structure can be expected for this alloy. This may explain why alloys 5083 and 5383 have approximatively the same resistance to exfoliation : the intergranular corrosion superiority of 5383 is balanced out by its more elongated grain structure.

As regards natural exposure behaviour, 5383 performs significantly better than 5083. The alloys exposed to marine atmosphere and immersion have not been artificially aged, which is relevant given the application. This is why only pitting, without exfoliation nor intergranular corrosion, is observed after 1 and 2 years of natural exposure.

As regards pitting corrosion, it is well known [8] that it is a localised corrosion phenomenon which results, for aluminium alloys, from a local breakdown of the passive oxyde film. Pitting propagation is an electrochemical process that consists of an anodic reaction (dissolution of aluminium) coupled with a cathodic oxygen and water reduction process that is the limiting factor. It takes place at cathodic sites which are generally the large surface incoherent intermetallics that stem from the solidification stage : α-AlFeMnSi, Al_6(Mn,Fe), Al_3Fe.

Amoung those, Al_3Fe intermetallics are the most detrimental to the pitting resistance. Since 5383 has a higher purity (lower iron and silicon contents) than 5083, it contains less cathodic sites which could explain why it performs better with respect to pitting corrosion. Calculation of the microstructure obtained at the end of the solidification stage show that the amount of Al_3Fe intermetallics is four times higher for 5083 than 5383.

The more elongated grain structure of 5383 might also be a beneficial factor with respect to the pitting resistance [8].

5. CONCLUSION

1 - Like conventional AA5083, alloy AA5383 which displays a higher yield strength after welding, is not sensitive to structural corrosion (intergranular, exfoliation, SCC) in the as-received temper. After accelerated ageing, these two alloys may become sensitive. However, as regards intergranular and stress corrosion, the new alloy 5383 performs significantly better than conventional 5083. As regards exfoliation, the two alloys have the same behaviour.

2 - To account for these observations, the following mechanism is proposed : owing to its high manganese and purity levels, 5383 contains more manganese-rich dispersoids. These dispersoids perturb the continuous grain boundary precipitation of magnesium that occurs during ageing, thus reducing the rate of sensitisation to intergranular corrosion. This entails a better SCC resistance, SCC and intergranular corrosion being closely related. However, 5383 displays a more elongated grain structure, which explains that it does not perform better than 5083 with respect to exfoliation corrosion.

3 - 5383 also exhibits a better resistance to pitting corrosion than 5083 after natural exposure tests. This might be due to its lower iron content and to a more elongated grain structure.

REFERENCES

[1] D.O. Sprowls and R.H. Brown. Proceedings of "Fundamental aspects of SCC". Edited by R.W. Staehle, A.J. Forty and D. van Rooynen. NACE, Houston, Texas, 1967.

[2] E.H. Hollinsworth and H.Y. Hunsicker. "Metals Handbook vol. 13". ASM, Metals Park, Ohio, 1987.

[3] International patent application WO 96/26299. Pechiney Rhenalu.

[4] G.M. Raynaud. "Changing aluminium products in the marine market". 12th fast ferry international conference. Copenhaguen, Denmark, 1996.

[5] Journal Officiel des Communautés Européennes N° C104-84 to 89, 1974.

[6] E.H. Dix, W.A. Anderson and M.B. Shumaker. Alcoa technical paper N°14, 1958.

[7] C. Sigli, H. Vichery and B. Grange. Materials Science Forum, vol. 217-222, 1996.

[8] M. Reboul, T. Warner, H. Mayet and B. Baroux. Corrosion Reviews, vol. 15, N° 3-4, 1997.

ACKNOWLEDGEMENTS

Thanks are due to Pechiney Rhenalu for permission to publish, to M. Durand and I. Bédènes for conducting the corrosion trials, to A. Reeves for performing the TEM observations and to C. Sigli for the thermodynamic calculations.